Biochemical and Biophysical Research Communications 450 (2014) 948–952

Contents lists available at ScienceDirect

Biochemical and Biophysical Research Communications

journal homepage: www.elsevier.com/locate/ybbrc

Single-reversal charge in the β10-β11 receptor-binding loop of *Bacillus thuringiensis* Cry4Aa and Cry4Ba toxins reflects their different toxicity against *Culex* spp. larvae

Sarinporn Visitsattapongse [a,b], Somsri Sakdee [b], Somphob Leetacheewa [b], Chanan Angsuthanasombat [b,c,*]

[a] Department of Clinical Chemistry, Faculty of Medical Technology, Mahidol University, Nakornpathom 73170, Thailand
[b] Bacterial Protein Toxin Research Unit, Institute of Molecular Biosciences, Mahidol University, Nakornpathom 73170, Thailand
[c] Laboratory of Molecular Biophysics and Structural Biochemistry, Biophysics Institute for Research and Development (BIRD), Bangkok 10150, Thailand

ARTICLE INFO

Article history:
Received 14 June 2014
Available online 24 June 2014

Keywords:
Bacillus thuringiensis
Cry4 toxins
Receptor-binding loop
Charge-reversal mutation
Culex mosquito-larvae

ABSTRACT

Bacillus thuringiensis Cry4Aa toxin was previously shown to be much more toxic to *Culex* mosquito-larvae than its closely related toxin – Cry4Ba, conceivably due to their sequence differences within the β10-β11 receptor-binding loop. Here, single-Ala substitutions of five residues (Pro^{510}, Thr^{512}, Tyr^{513}, Lys^{514} and Thr^{515}) within the Cry4Aa β10-β11 loop revealed that only Lys^{514} corresponding to the relative position of Cry4Ba-Asp^{454} is crucial for toxicity against *Culex quinquefasciatus* larvae. Interestingly, charge-reversal mutations at Cry4Ba-Asp^{454} (D454R and D454K) revealed a marked increase in toxicity against such less-susceptible larvae. *In situ* binding analyses revealed that both Cry4Ba-D454R and D454K mutants exhibited a significant increase in binding to apical microvilli of *Culex* larval midguts, albeit at lower-binding activity when compared with Cry4Aa. Altogether, our present data suggest that a positively charged side-chain near the tip of the β10-β11 loop plays a critical role in determining target specificity of Cry4Aa against *Culex* spp., and hence a great increase in the *Culex* larval toxicity of Cry4Ba was obtained toward an opposite-charge conversion of the corresponding Asp^{454}.

1. Introduction

During the past several decades, the entomopathogenic bacterium *Bacillus thuringiensis* (*Bt*), particularly *Bt* subsp. *israelensis* (*Bti*), has become one of the most promising bioinsecticides for the control of mosquito-disease vectors which are annually responsible for the transmission of parasitic and viral infections to millions of people worldwide [1–4]. *Bti* produces insecticidal crystal inclusions consisting of both crystalline (Cry) and cytolytic (Cyt) δ-endotoxins, *i.e.* Cry4Aa (~130 kDa), Cry4Ba (~130 kDa), Cry11Aa (~65 kDa) and Cyt1Aa (~27 kDa), which are, to various extents, toxic to mosquito larvae of three medically important genera, *Aedes*, *Anopheles* and *Culex* [1–3]. For instance, the two closely related 130-kDa *Bti* toxins – Cry4Aa and Cry4Ba display comparable toxicity against both *Aedes* and *Anopheles* larvae, but the Cry4Aa toxin is much more toxic to *Culex* larvae [5].

The native *Bt*-Cry δ-endotoxins are synthesized as inactive protoxins that are found within parasporal crystalline inclusions. Once ingested by susceptible insect larvae, the Cry toxin inclusions are dissolved under alkaline conditions of the larval midgut lumen where the soluble protoxins are then cleaved by gut digestive proteases to yield ~65-kDa active portions that are relatively resistant to further proteolysis [2,6,7]. The activated toxins are believed to first interact specifically with a variety of membrane components (so-called receptors) located on the surface of the midgut epithelial cells [6–8]. For example, in our previous findings, two different membrane-bound proteins, *i.e.* GPI (glycosylphosphatidylinositol)-anchored aminopeptidases-N and GPI-anchored alkaline phosphatases, were identified as potential receptors mediating toxicity for Cry4Ba in *Aedes* larvae [9–11]. The toxin-receptor interactions would facilitate toxin insertion into the cell membrane to form ion-leakage pores, resulting in cell lysis and eventual death of the target insect larvae [6–8]. Nonetheless, the exact toxic mechanism underlying the specific effect at the molecular level of each individual toxin still remains to be explored.

We currently know the X-ray crystal structures of numerous *Bt*-Cry toxins [12–16], including the two mosquito-active toxins – Cry4Aa and Cry4Ba [15,16]. All these 65-kDa activated toxin

* Corresponding author at: Bacterial Protein Toxin Research Unit, Institute of Molecular Biosciences, Mahidol University, Nakornpathom 73170, Thailand. Fax: +66 2 4419906.
E-mail address: chanan.ang@mahidol.ac.th (C. Angsuthanasombat).

http://dx.doi.org/10.1016/j.bbrc.2014.06.090
0006-291X/

structures reveal a wedge-shaped form consisting of three structurally and functionally distinctive domains which are, from the N- to C-terminus, a bundle of α-helices (DI), a three-β-sheet domain (DII) and a β-sandwich (DIII). Despite the fact that both Cry4Aa and Cry4Ba structures bear a likeness to the other *Bt*-Cry structures, their finer features are rather dissimilar as there is additional *in vitro* proteolysis by trypsin occurring at Cry4Aa-Arg^{235} or Cry4Ba-Arg^{203} located in the α5-α6 loop within DI, generating two non-covalently associated fragments of ~47 and ~20 kDa [17,18]. Thus far, although the precise role of the C-terminal DIII is not yet evidently elucidated, the N-terminal α-helical bundle – DI and the β-sheet prism – DII have been clearly demonstrated to be membrane pore-forming and receptor-binding domains, respectively [2,7].

In our previous studies, the role in toxicity for DI and DII of both Cry4Aa and Cry4Ba has been intensively investigated (for reviews, *see* [2]). Very recently, we have demonstrated the functional importance of intrinsic stability toward the Pro-rich cluster (Pro^{193}Pro^{194}_Pro^{196}) which is present exclusively in the Cry4Aa-long loop connecting the two pore-lining helices – α4 and α5 [19]. We have also signified that the polarity of the Cry4Ba α4-α5 loop residue – Asn^{166} is implicated in ion permeation through the toxin-induced pore and likely to promote the toxin-pore opening [20]. For a functional role in receptor binding of DII, while most other workers' studies are restricted to only three β-hairpin loops, *i.e.* β2-β3, β6-β7 and β10-β11 loops (originally assigned as loops 1, 2 and 3, respectively), we have shown that two other Cry4Ba-loops, *i.e.* β4-β5 and β8-β9 loops, are also implicated in receptor binding [21,22]. More recently, we have demonstrated that the Cry4Ba toxin specifically utilizes two receptor-binding loops – β2-β3 and β4-β5 loops to interact with its alternative receptor-Cyt2Aa2 for synergistic activity against *Aedes* larvae [23]. In the present study, we have provided critical evidence for functional implications of one oppositely charged side-chain, *i.e.* Cry4Aa-Lys^{514} and Cry4Ba-Asp^{454}, located within the β10-β11 receptor-binding loop (*see* Fig. 1) in view of the fact that these two closely related *Bti* toxins are toxic to *Culex* mosquito-larvae at greatly different degrees of toxicity.

2. Materials and methods

2.1. Constructions of mutant plasmids

pMEx-B4A recombinant plasmid, encoding the 130-kDa Cry4Aa toxin under control of the *tac* promoter in combination with the *cry4Ba* promoter [24], was used as a template for single-Ala substitutions of β10-β11 loop residues (Fig. 1A). p4Ba-R203Q plasmid, encoding the 130-kDa Cry4Ba-R203Q mutant toxin in which one trypsin-cleavage site at Arg^{203} was removed [25], was used as a template for targeted mutations at Asp^{454} within the β10-β11 loop. Complementary mutagenic primers (*see* Supplementary Table 1) were designed according to the published *cry4Aa* and *cry4Ba* gene sequences [26,27]. All loop-mutant plasmids were generated by PCR-based directed mutagenesis using a high-fidelity Phusion DNA polymerase (Thermo Scientific), following the QuickChange™ mutagenesis procedure (Stratagene). Selected mutant clones were first identified by restriction endonuclease analysis and then verified by DNA sequencing (Macrogen, Inc., Korea).

2.2. Expression and partial purification of toxin inclusions

Cry4Aa and Cry4Ba toxins were over-expressed in *Escherichia coli* strain JM109 as inclusions upon 4-h induction with isopropyl-β-D thiogalactopyranoside (IPTG, 0.1 mM final concentration). Cells expressing each individual toxin were disrupted by using a French Pressure Cell (10,000 psi) and the inclusions were partially purified from cell lysate by centrifugation (6000*g* for 10 min at 4 °C) and washing as described earlier [19]. Protein concentrations of partially purified inclusions were determined with the Bradford-based protein microassay (Bio-Rad), using bovine serum albumin (fraction V, Sigma) as a calibration standard.

2.3. Solubilization of inclusions and proteolytic digestion of protoxins

Individual toxin inclusions (~1 mg/mL) were solubilized in 50 mM Na_2CO_3/$NaHCO_3$ (pH 10.0) at 37 °C for 1 h as previously described [19]. Following centrifugation (6000*g*, 10 min, 4 °C), supernatants containing soluble toxins were subjected to SDS-PAGE analysis in comparison with their corresponding inclusion suspensions. Each soluble protoxin was then tested for their proteolytic stability by digestion with trypsin (L-1-tosylamido-2-phenylethyl chloromethyl ketone-treated, Sigma) at a ratio of 1:20 enzyme/toxin (w/w) in the carbonate buffer (pH 10.0) for 16 h at 37 °C prior to SDS-PAGE analysis.

2.4. Assessment of larvicidal activity of mutant toxins

To determine mutational effects on toxicity of mutant toxins, bioassays were performed by using 2–5 day-old *C. quinquefasciatus* mosquito-larvae. Larvae were fasted for 2–4 h before beginning the assays performed using 24-multi-well plates (Costar) with twenty larvae per well containing 2-mL aqueous suspension of *E. coli* expressing each toxin (~2×10^8 cells). Larval mortality was recorded after 24-h incubation period at room temperature. Statistical analyses were performed by using *t-test* function *via* the Excel software (Microsoft) for determining the significance differences between mutants and the Wt.

2.5. Immuno-histochemical binding assays

Sections of paraffin-embedded histological tissues were prepared from 5 day-old *C. quinquefasciatus* mosquito-larvae pre-fed with individual tested toxins (~10 μg/mL per larvae) and immuno-histochemical staining was accomplished following the method described earlier [28]. For detection of bound toxins, the larval sections were sequentially probed with rabbit anti-specific toxin polyclonal antibodies (1:100 dilution), biotin-conjugated goat anti-rabbit IgGs (1:8000 dilution) and peroxidase-conjugated streptavidin (1:50,000 dilution). Color was finally developed with a 3,3′-diaminobenzidine-peroxidase substrate (SK-4100, Vector Labs).

3. Results and discussion

3.1. Involvement in Culex toxicity of Cry4Aa-Lys^{514} located in the β10-β11 loop

In the present study, we started to explore a possible involvement of the β10-β11 loop of Cry4Aa in *Culex* toxicity and five Ala-substituted mutants (*i.e.* P510A, T512A, Y513A, K514A and T515A) were initially constructed. Upon IPTG-induction, all mutants were over-expressed in *E. coli* as cytoplasmic inclusions, yielding the 130-kDa mutant protoxins at levels about the same as the Cry4Aa-Wt toxin (*see* Supplementary Fig. 1A). When mutant inclusions were assessed for their solubility *in vitro*, all were found to be highly soluble in the carbonate buffer (pH 10.0), giving >90% solubility which is comparable to that of the Wt toxin (*see* Supplementary Fig. 1C). We also examined for trypsin digestion susceptibility of the mutant protoxins as a presumptive assessment of overall folding fidelity. All the 130-kDa soluble mutant toxins were

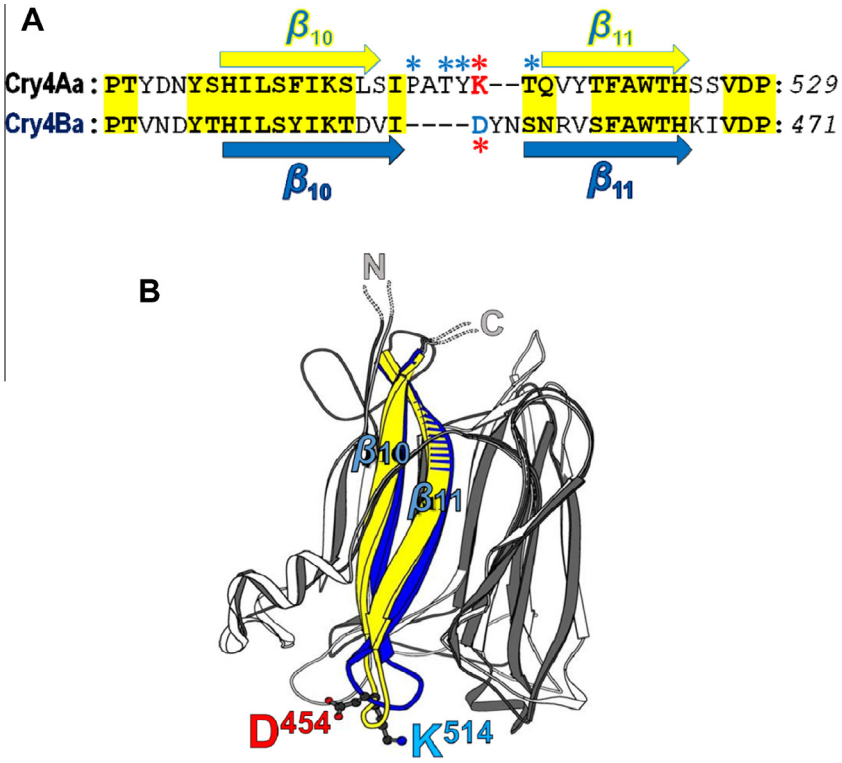

Fig. 1. (A) Pairwise sequence alignment derived from B of the β10-β11 receptor-binding loop of Cry4Aa with that of its closely related toxin – Cry4Ba. Corresponding β-strands of Cry4Aa and Cry4Ba are illustrated over and under the sequences, respectively. Mutated residues (Cry4Aa: Pro^{510}, Thr^{512}, Tyr^{513}, Lys^{514} and Thr^{515}; Cry4Ba: Asp^{454}) are indicated by *. (B) Superimposition of Cry4Aa-DII (shaded yellow/white) and Cry4Ba-DII (shaded blue/gray) crystal structures, revealing that Cry4Aa-Lys^{514} and Cry4Ba-Asp^{454} correspond to each other and give the sequence alignment in A. All structures were generated by using MOLSCRIPT and PyMOL programs. (For interpretation of the references to color in this figure legend, the reader is referred to the web version of this article.)

found to produce two major trypsin-resistant fragments of ~47 and ~21 kDa as corresponding to the trypsin-treated Wt toxin (*see* Supplementary Fig. 1C). This could indicate that all these mutants were produced as structurally stable protoxins and that each individual mutation introduced into the Cry4Aa β10-β11 loop had no apparent effect on the structural characteristic of the mutant protoxins.

E. coli cells expressing each Cry4Aa-loop mutants were then examined for their toxicity against *C. quinquefasciatus* larvae. It was found that only the K514A mutant exhibited a marked decrease in larvicidal activity (~50% of the Wt value) while four other mutants (P510A, T512A, Y513A and T515A) still retained the high larval toxicity (Fig. 2). These results suggested that Cry4Aa-Lys^{514} located within the β10-β11 loop is basically involved in toxin activity against *Culex* larvae. However, our previous replacement of this critical residue with Asn (K514N) showed no effect on toxicity against *C. quinquefasciatus* larvae [15], indicating that the uncharged polar character of an Asn side-chain is sufficient to compensate for the Cry4Aa-Lys^{514} residue. Besides, our data demonstrated here are rather contrary to other related studies where Ala-substitutions at Thr^{512} and Tyr^{513}, but not Lys^{514}, in the Cry4Aa β10-β11 loop were claimed to have an adverse effect on toxin activity against *Culex pipiens* mosquito-larvae [29]. This apparent discrepancy of the mutational effects observed between *C. quinquefasciatus* and *C. pipiens* might reflect different types of target receptors for Cry4Aa present in these two *Culex* species.

3.2. Effects on Culex toxicity of charge-reversal mutations at Cry4Ba-Asp^{454}

Although we have shown previously that the Ala-substitution of Cry4Ba-Asp^{454} showed no effect on toxin activity against *Aedes*

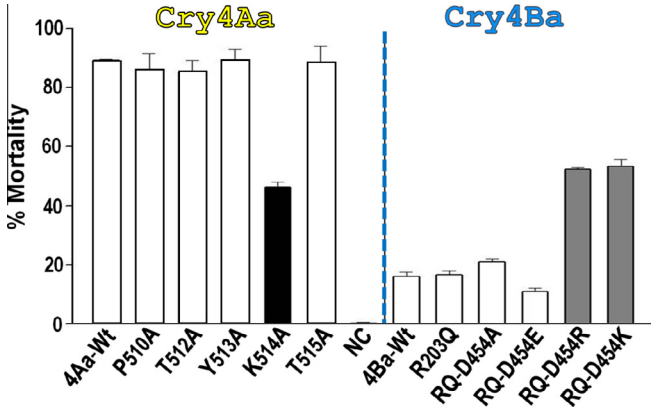

Fig. 2. Larvicidal activities of *E. coli* cells (~10^8 cells/ml) expressing Cry4Aa, Cry4Ba or their mutant toxins against *C. quinquefasciatus* mosquito-larvae. Cells harboring the pMEx-8 vector were used as a negative control (NC). Error bars indicate standard errors of the mean from at least three independent experiments. Shaded graphs represent larval toxicity of the K514A mutant (left panel), and RQ-D454R and RQ-D454K mutants (right panel) that are marked different (p values <0.01) from that of their Wt-toxins.

larvae [21], it was still interesting to check whether this residue which is located within the β10-β11 loop has an adverse effect on *Culex* toxicity since Cry4Ba is very less active toward *Culex* species than Cry4Aa. Moreover, it can be clearly inferred from the superimposed Cry4-DII structures (Fig. 1B) that the position of Cry4Ba-Asp^{454} is located in close proximity to that of Cry4Aa-Lys^{514} which was demonstrated above to be crucial for *Culex* toxicity (*see* Fig. 2). Attempts were therefore made to convert the negatively charged nature of Cry4Ba-Asp^{454} to be a positive charge corresponding to Cry4Aa-Lys^{514}. In this context, Asp^{454} of the

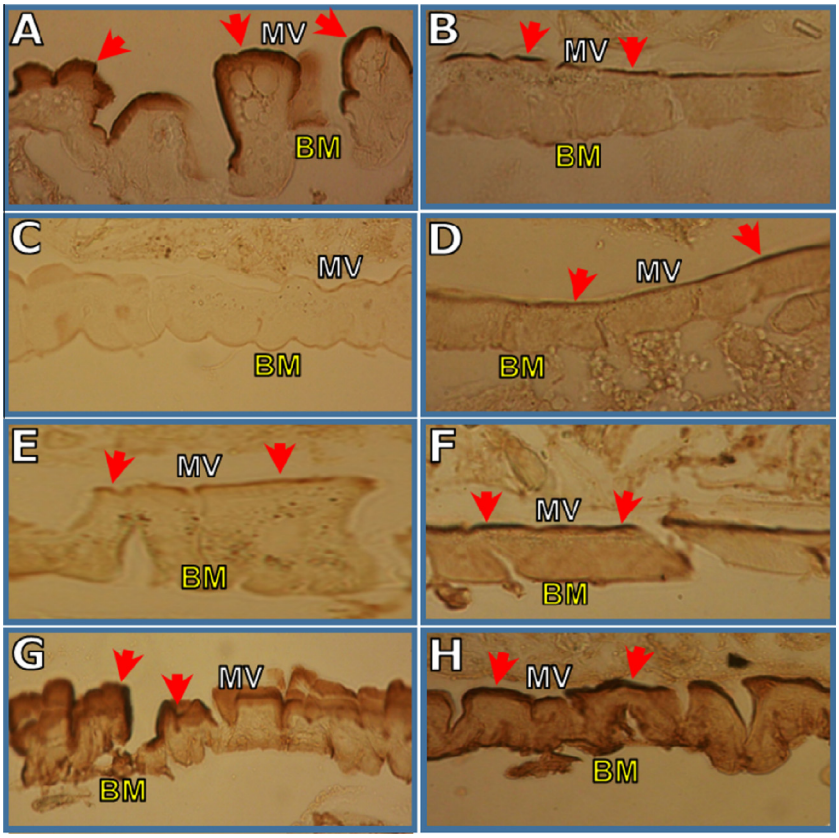

Fig. 3. Immuno-histochemical staining of 5-day-old *C. quinquefasciatus* larval posterior midgut sections that were prepared from individual mosquito-larvae pre-fed with toxin inclusions of either (A) Cry4Aa-Wt, (B) Cry4Ba-Wt, (D) Cry4Ba-R203Q, (E) RQ-D454E, (F) RQ-D454A, (G) RQ-D454R or (H) RQ-D454K. (C) Control slide omitting the tested proteins. Arrows indicate apical microvilli (MV). BM, basement membrane.

Cry4Ba-R203Q mutant toxin (RQ), which retained high *Aedes* toxicity and produced a 65-kDa active fragment upon trypsin digestion [25], was further mutated to Lys, Arg, Ala or Glu. All four constructed RQ mutants, *i.e.* RQ-D454K, RQ-D454R, RQ-D454A and RQ-D454E, were found to be highly expressed in *E. coli* cells as inclusion bodies which could be easily solubilized in the carbonate buffer (pH 10.0) and cleaved by trypsin to yield a single fragment of ~65 kDa similar to the RQ template toxin (*see* Supplementary Fig. 1B, D).

Interestingly, when *E. coli* cells expressing each Cry4Ba mutant toxin were tested for their relative bioactivity against *Culex* larvae, both charge-reversal mutants, *i.e.* RQ-D454R and RQ-D454K, displayed a striking increase in larval toxicity compared to Cry4Ba-Wt and RQ-template (Fig. 2). However, the RQ-D454E mutant showed a significant reduction of *Culex* toxicity while the D454A mutant displayed a little positive effect on the larval toxicity (Fig. 2). These results suggested that the positively charged character of Cry4Ba-residue^{166} corresponding relatively to the position of Cry4Aa-Lys^{514} near the tip of the β10-β11 loop is indispensable for *Culex* larvicidal activity.

Our present data are in agreement to a certain extent with that of Abdullah *et al.* [30] which also showed that replacements of Cry4Ba-Asp^{454} with a particular variety of tripeptides (*e.g.* PAT, AAT, GAT, GAV and PAA, but not AAA) can enhance toxin activity toward *C. quinquefasciatus* larvae. However, the authors suggested that the specific amino acid sequence in the β10-β11 loop is not crucial for *Culex* larval toxicity, although their mutations at Cry4Ba-Asp^{454} have not been done yet with a charged residue [30]. More recently, a similar positive consequence was observed for GluA2 (ligand-gated ionotropic glutamate/AMPA receptors) when a charge-reversal mutation (R628E) at Arg^{628} located in its linker region caused an increase in ligand-binding affinity [31].

3.3. Effects of charge-reversal mutations at Cry4Ba-Asp^{454} on binding to Culex larval midguts

Attempts were further made to determine whether the positive consequence toward *Culex* toxicity of the two charge-reversal mutants (*i.e.* RQ-D454R and RQ-D454K) is correlated with their efficiency in binding to the target receptors. Our previous binding studies *via* immuno-histochemical staining showed that the primary site of action of Cry4Ba or its mutant toxins is located at the apical microvilli of *Aedes* larval posterior midguts [22,23,28]. Herein, *in situ* binding analyses revealed that both RQ-D454R and RQ-D454K mutants exhibited a marked increase in their binding to the apical brush-border of *Culex* midguts (Fig. 3G,H) when compared with Cry4Ba-Wt and RQ-template (Fig. 3B,D). The results also revealed that while the RQ-D454A mutant showed no noticeable increase in binding (Fig. 3F), the retained negatively-charged mutant (*i.e.* RQ-D454E) exhibited an apparent decrease in the immunochemical signal detected on the apical-brush border of posterior midgut sections (Fig. 3E). As expected, Cry4Aa which is much higher toxic than Cry4Ba toward *Culex* larvae showed an intense-brown staining along the apical microvilli of *Culex* epithelial cells (Fig. 3A). However, the control larval gut section in which a test toxin was omitted displayed a very weak staining of non-specific signals on the larval microvilli (Fig. 3C). These results corroborated the potential involvement in receptor binding through an increased *Culex* toxicity of an introduced positive charge at the Cry4Ba-position^{454} placed within the β10-β11 loop. As demonstrated above, Cry4Aa-Lys^{514} whose position corresponds relatively to Cry4Ba-Asp^{454} was essentially implicated in *Culex* toxicity. Thereby, it is reasonable to postulate that the positively charged character at this corresponding loop-position, Cry4Aa-position^{514} and Cry4Ba-position^{454}, is involved in ionic interactions

with the negatively charged counterpart of a *Culex* membrane-receptor.

Acknowledgments

This work was supported in part by grants from the Thailand Research Fund (grant number BRG-53-8-0007) in cooperation with the Commission of Higher Education (CHE), Ministry of Education (Thailand). A scholarship from CHE (to S.V.) is gratefully acknowledged. We also thank Ms. Pensri Hongthong for technical assistance. Thanks are also due to the reviewers for their constructive critiques.

Appendix A. Supplementary data

Supplementary data associated with this article can be found, in the online version, at http://dx.doi.org/10.1016/j.bbrc.2014.06.090.

References

[1] B.A. Federici, H.-W. Park, D.K. Bideshi, Overview of the basic biology of *Bacillus thuringiensis* with emphasis on genetic engineering of bacterial larvicides for mosquito control, Open Toxinol. J. 3 (2010) 83–100.
[2] C. Angsuthanasombat, Structural basis of pore formation by mosquito-larvicidal proteins from *Bacillus thuringiensis*, Open Toxinol. J. 3 (2010) 119–125.
[3] E. Ben-Dov, *Bacillus thuringiensis* subsp. *israelensis* and its dipteran-specific toxins, Toxins 6 (2014) 1222–1243.
[4] L. Regis, M.H. Silva-Filha, C. Nielsen-LeRoux, J.F. Charles, Bacteriological larvicides of dipteran disease vectors, Trends Parasitol. 17 (2001) 377–380.
[5] C. Angsuthanasombat, N. Crickmore, D.J. Ellar, Comparison of *Bacillus thuringiensis* subsp. *israelensis* CryIVA and CryIVB cloned toxins reveals synergism in vivo, FEMS Microbiol. Lett. 94 (1992) 63–68.
[6] E. Schnepf, N. Crickmore, J. van Rie, D. Lereclus, J. Baum, J. Feitelson, D.R. Zeigler, D.H. Dean, *Bacillus thuringiensis* and its pesticidal crystal proteins, Microbiol. Mol. Biol. Rev. 62 (1998) 775–806.
[7] L. Pardo-López, M. Soberón, A. Bravo, *Bacillus thuringiensis* insecticidal three-domain Cry toxins: mode of action, insect resistance and consequences for crop protection, FEMS Microbiol. Rev. 37 (2013) 3–22.
[8] C.R. Pigott, D.J. Ellar, Role of receptors in *Bacillus thuringiensis* crystal toxin activity, Microbiol. Mol. Biol. Rev. 71 (2007) 255–281.
[9] M. Dechklar, K. Tiewsiri, C. Angsuthanasombat, K. Pootanakit, Functional expression in insect cells of glycosylphosphatidylinositol-linked alkaline phosphatase from *Aedes aegypti* midgut larvae: a *Bacillus thuringiensis* Cry4Ba toxin-receptor, Insect Biochem. Mol. Biol. 41 (2010) 159–166.
[10] M. Saengwiman, A. Aroonkesorn, S. Sakdee, S. Leetachewa, C. Angsuthanasombat, K. Pootanakit, In vivo identification of *Bacillus thuringiensis* Cry4Ba toxin receptors by RNA interference knockdown of glycosylphosphatidylinosiol-linked aminopeptidase N transcripts in *Aedes aegypti* larvae, Biochem. Biophys Res. Commun. 407 (2011) 708–713.
[11] A. Thammasittirong, M. Dechklar, S. Leetachewa, K. Pootanakit, C. Angsuthanasombat, *Aedes aegypti* membrane-bound alkaline phosphatase expressed in *Escherichia coli* retains high-affinity binding for *Bacillus thuringiensis* Cry4Ba toxin, Appl. Environ. Microbiol. 77 (2011) 6836–6840.
[12] P. Grochulski, L. Masson, S. Borisova, M. Pusztai-Carey, J.-L. Schwartz, R. Brousseau, M. Cygler, *Bacillus thuringiensis* CrylA(a) insecticidal toxin: crystal structure and channel formation, J. Mol. Biol. 254 (1995) 447–464.
[13] R.J. Morse, T. Yamamoto, R.M. Stroud, Structure of Cry2Aa suggests an unexpected receptor binding epitope, Structure 9 (2001) 409–417.
[14] J. Li, J. Carroll, D.J. Ellar, Crystal structure of insecticidal δ-endotoxin from *Bacillus thuringiensis* at 2.5 Å resolution, Nature 353 (1991) 815–821.
[15] P. Boonserm, M. Mo, C. Angsuthanasombat, J. Lescar, Structure of the functional form of the mosquito larvicidal Cry4Aa toxin from *Bacillus thuringiensis* at a 2.8-angstrom resolution, J. Bacteriol. 188 (2006) 3391–3401.
[16] P. Boonserm, P. Davis, D.J. Ellar, J. Li, Crystal structure of the mosquito-larvicidal toxin Cry4Ba and its biological implications, J. Mol. Biol. 348 (2005) 363–382.
[17] C. Angsuthanasombat, N. Crickmore, D.J. Ellar, Effects on toxicity of eliminating a cleavage site in a predicted interhelical loop in *Bacillus thuringiensis* CryIVB delta endotoxin, FEMS Microbiol. Lett. 111 (1993) 255–261.
[18] C. Angsuthanasombat, P. Uawithya, S. Leetachewa, W. Pornwiroon, P. Ounjai, T. Kerdcharoen, G. Katzenmeier, S. Panyim, *Bacillus thuringiensis* Cry4A and Cry4B mosquito-larvicidal proteins: homology-based 3D model and implications for toxin activity, J. Biochem. Mol. Biol. 37 (2004) 304–313.
[19] C. Imtong, C. Karnchanawarin, G. Katzenmeier, C. Angsuthanasombat, C. *Bacillus thuringiensis* Cry4Aa insecticidal protein: functional importance of intrinsic stability of the unique α4-α5 loop comprising the Pro-rich sequence, Biochim. Biophys. Acta Proteins Proteomics 1844 (2014) 1111–1118.
[20] T. Juntadech, Y. Kanintronkul, C. Kanchanawarin, G. Katzenmeier, C. Angsuthanasombat, Importance of polarity of the α4-α5 loop residueAsn166 in the pore-forming domain of the *Bacillus thuringiensis* Cry4Ba toxin: implications for ion permeation and pore opening, Biochim. Biophys. Acta Biomembr. 1838 (2014) 319–327.
[21] T. Tuntitippawan, P. Boonserm, G. Katzenmeier, C. Angsuthanasombat, Targeted mutagenesis of loop residues in the receptor-binding domain of the *Bacillus thuringiensis* Cry4Ba toxin affects larvicidal activity, FEMS Microbiol. Lett. 242 (2005) 325–332.
[22] T. Khaokhiew, C. Angsuthanasombat, C. Promptmas, Correlative effect on the toxicity of three surface-exposed loops in the receptor-binding domain of the *Bacillus thuringiensis* Cry4Ba toxin, FEMS Microbiol. Lett. 300 (2009) 139–145.
[23] C. Lailak, T. Khaokhiew, C. Promptmas, B. Promdonkoy, K. Pootanakit, C. Angsuthanasombat, *Bacillus thuringiensis* Cry4Ba toxin employs two receptor-binding loops for synergistic interactions with Cyt2Aa2, Biochem. Biophys. Res. Commun. 435 (2013) 216–221.
[24] P. Boonserm, W. Pornwiroon, G. Katzenmeier, S. Panyim, C. Angsuthanasombat, Optimised expression in *Escherichia coli* and purification of the functional form of the *Bacillus thuringiensis* Cry4Aa δ-endotoxin, Protein Expr. Purif. 35 (2004) 397–403.
[25] N. Thamwiriyasati, S. Sakdee, P. Chuankhayan, G. Katzenmeier, C.J. Chen, C. Angsuthanasombat, Crystallization and preliminary X-ray crystallographic analysis of a full-length active form of Cry4Ba toxin from *Bacillus thuringiensis*, Acta Crystallogr. F 66 (2010) 721–724.
[26] C. Angsuthanasombat, W. Chungjatupornchai, S. Kertbundit, P. Luxananil, C. Settasatian, P. Wilairat, S. Panyim, Cloning and expression of 130-kd mosquito-larvicidal delta-endotoxin gene of *Bacillus thuringiensis* var. *israelensis* in *Escherichia coli*, Mol. Gen. Genet. 208 (1987) 384–389.
[27] E.S. Ward, D.J. Ellar, Nucleotide sequence of a *Bacillus thuringiensis* var. *israelensis* gene encoding a 130 kDa delta-endotoxin, Nucleic Acids Res. 15 (1987) 7195.
[28] P. Chayaratanasin, S. Moonsom, S. Sakdee, U. Chaisri, G. Katzenmeier, C. Angsuthanasombat, High level of soluble expression in *Escherichia coli* and characterisation of the cloned *Bacillus thuringiensis* Cry4Ba domain III fragment, J. Biochem. Mol. Biol. 40 (2007) 58–64.
[29] M.T.H. Howlader, Y. Kagawa, A. Miyakawa, A. Yamamoto, T. Taniguchi, T. Hayakawa, H. Sakai, Alanine scanning analyses of the three major loops in domain II of *Bacillus thuringiensis* mosquitocidal toxin Cry4Aa, Appl. Environ. Microbiol. 76 (2010) 860–865.
[30] M.A.F. Abdullah, O. Alzate, M. Mohammad, R.J. McNall, M.J. Adang, D.H. Dean, Introduction of *Culex* toxicity into *Bacillus thuringiensis* Cry4Ba by protein engineering, Appl. Environ. Microbiol. 69 (2003) 5343–5353.
[31] J.E. Harms, M. Benveniste, M. Kessler, L.M. Stone, A.C. Arai, K.M. Partin, A charge-inverting mutation in the linker region of a-amino-3-hydroxy-5-methyl-4-isoxazolepropionic acid (AMPA) receptors alters agonist binding and gating kinetics independently of allosteric modulators, J. Biol. Chem. 289 (2014) 10702–10714.